Downscaling Climate over Complex Terrain: High Finescale (<1000 m) Spatial Variation of Near-Ground Temperatures in a Montane Forested Landscape (Great Smoky Mountains)*

JASON D. FRIDLEY

Department of Biology, University of North Carolina at Chapel Hill, Chapel Hill, North Carolina, and Department of Biology, Syracuse University, Syracuse, New York

(Manuscript received 18 July 2008, in final form 9 October 2008)

ABSTRACT

Landscape-driven microclimates in mountainous terrain pose significant obstacles to predicting the response of organisms to atmospheric warming, but few if any studies have documented the extent of such finescale variation over large regions. This paper demonstrates that ground-level temperature regimes in Great Smoky Mountains National Park (Tennessee and North Carolina) vary considerably over fine spatial scales and are only partially linked to synoptic weather patterns and environmental lapse rates. A 120-sensor network deployed across two watersheds in 2005–06 exhibited finescale (<1000-m extent) temperature differences of over 2°C for daily minima and over 4°C for daily maxima. Landscape controls over minimum temperatures were associated with finescale patterns of soil moisture content, and maximum temperatures were associated with finescale insolation differences caused by topographic exposure and vegetation cover. By linking the sensor array data to 10 regional weather stations and topographic variables describing site radiation load and moisture content, multilevel spatial models of 30-m resolution were constructed to map daily temperatures across the 2090-km^2 park, validated with an independent 50-sensor network. Maps reveal that different landscape positions do not maintain relative differences in temperature regimes across seasons. Near-stream locations are warmer in the winter and cooler in the summer, and sites of low elevation more closely track synoptic weather patterns than do wetter high-elevation sites. This study suggests a strong interplay between near-ground heat and water balances and indicates that the influence of past and future shifts in regional temperatures on the park's biota may be buffered by soil moisture surfeits from high regional rainfall.

1. Introduction

A major obstacle to predicting how ecological communities will react to a warming atmosphere is that most organisms do not directly interact with the atmosphere but rather respond to the properties of their near-ground microenvironment, which are tempered by finescale differences in landform, substrate, and vegetation (Geiger et al. 2003). The need for such climate ''downscaling'' has been voiced repeatedly by environmental scientists (e.g., Araújo et al. 2005; Trivedi et al. 2008), and yet the extent of finescale (<1000 m) variation, and the principal landscape factors that contribute to it, remain poorly understood. In topographically complex montane environments, finescale variance in solar heat transfer due to varying slope angle and orientation, shading from local vegetation, and soil and plant water content can significantly alter the temperature regimes of locations only meters apart (Hursh 1948; Parker 1952; Shanks 1956; Barry 1992; Breshears et al. 1998; Geiger et al. 2003; Ashcroft et al. 2008). Adiabatic cooling with elevation and cold-air drainage add yet additional variance within landscapes that further decouples near-ground temperature regimes from regional atmospheric qualities (Shreve 1912; Barry 1992; Geiger et al. 2003). Weather station networks capture regional-scale climate variation and are thus well suited for describing the distribution and habits of organisms over large distances (e.g., Iverson and Prasad 1998),

* Supplemental information related to this paper is available at the Journals Online Web site: http://dx.doi.org/10.1175/2008JAMC2084.s1.

Corresponding author address: Jason D. Fridley, Syracuse University, Department of Biology, 107 College Place, Syracuse, NY 13244.
E-mail: fridley@syr.edu

DOI: 10.1175/2008JAMC2084.1

but their scarcity and general confinement to open sites limit their use for quantifying near-ground, finescale temperature patterns within complex landscapes (Barry 1992; Bolstad et al. 1998; Lookingbill and Urban 2003).

Topoclimatology, the study of how complex terrain influences local climate, provides a history of case studies of landscape properties that influence local temperature regimes [see reviews by Barry (1992) and Geiger et al. (2003)]. However, topoclimatological studies have generally proceeded along two complementary routes: in one, the interpolation of climate variables over complex terrain has been performed over broad (e.g., continental) extents and large spatial grains (e.g., 1 km^2; Dodson and Marks 1997; Thornton et al. 1997); in the other, interpolation has been performed within landscapes at fine grains (<50 m) but within single watersheds or relatively small areas (e.g., Lookingbill and Urban 2003; Chung and Yun 2004). Because of the usual tradeoffs associated with extensive versus intensive modeling, it has proven difficult to capture microtopographic influences on climate at a spatial resolution that captures the local climate regimes that organisms experience and, simultaneously, a spatial extent that covers regional climate differences associated with broad elevation gradients and synoptic weather patterns. As a result, biotic patterns such as species distributions in montane systems are still often modeled in relation to the easily measured variables of elevation and site exposure [but see Urban et al. (2000)]. The situation is particularly acute when considering consequences of climate change for the distribution of mountain organisms (Barry 2005). Because downscaled, organism-relevant maps of contemporary and historical temperature regimes remain unavailable, our understanding of how temperature regulates species distribution and behavior—now or in the future—remains poor.

This study documents how near-ground temperatures in a topographically complex, biotically rich landscape—Great Smoky Mountains National Park (GSMNP) in the southern Appalachian Mountains of Tennessee and North Carolina—vary over fine (30-m resolution) spatial scales, from single-slope facets (stream-to-ridge transects) to the extent of the entire 2090-km^2 park, for daily minima and maxima over the course of July 2005–October 2006. The primary objective in this paper is to demonstrate the capacity for complex landscapes to alter the climate regimes that most near-ground organisms experience and thus to provide guidelines to environmental scientists as to which landscape components (e.g., streamsides, ridges, low vs high elevations) have microclimates most decoupled from synoptic weather patterns. Secondarily, this paper demonstrates the feasibility of low-cost temperature sensor networks that, when combined with spatial modeling techniques in a GIS framework, can be used to describe temperature regimes at spatial scales of both fine grain and large extent. This paper describes the establishment of the 170-sensor GSMNP Temperature Network; presents a multilevel, mixed-effect linear modeling approach based on maximum likelihood that flexibly describes landscape processes that exhibit hierarchical structure and spatiotemporal autocorrelation; and presents how such models, once validated, allow finescale mapping of temperature for all of GSMNP, built on GIS-derived topographic variables. Digital maps from these analyses are available as online supplemental material to this paper. (The supplemental information referred to in this paper consists of an HTML page that serves to give context and easy links to various documents, figures, and map files that are referenced herein, along with those documents, figures, and map files themselves. The files can be downloaded in compressed format from the URL given on the title page of this paper.)

2. Methods

a. Great Smoky Mountains National Park

GSMNP encompasses 2090 km^2 of the Smoky and Balsam Mountain ranges near the southern terminus of the southern Appalachian Mountains in Tennessee and North Carolina (Fig. 1). The park includes about one-half (17) of all mountain peaks above 1830 m MSL (6000 ft) in the eastern United States, and the highest point (Clingmans Dome: 2024 m) is within 12 m of the highest elevation east of the Mississippi River. Mountain valleys around most of the park boundary surround the central massif and reach as low as 256 m MSL (840 ft) on the western border, and the relatively short distance between elevation extremes (6–12 km) produces a steep terrain of narrow ridges and rocky coves. Except for a few areas maintained as fields and meadows, primary and mature secondary forest vegetation covers a mantle typified by metamorphosed sedimentary rock. GSMNP lacks a climatic treeline (Cogbill et al. 1997), but most tree species reach their upper or lower climatic limits within the park (Shanks 1954). Synoptic weather patterns typically move into the park from the west; although Gaffin et al. (2007) suggest that air masses on the leeward (eastern) side of GSMNP are typically drier because of orographic precipitation as air masses move eastward across the high peaks, long-term low-elevation precipitation differences around the park are minor. For seasons, precipitation is slightly higher in summer (July–August) and winter (November–January), and the water content of air and ground greatly reduces environmental

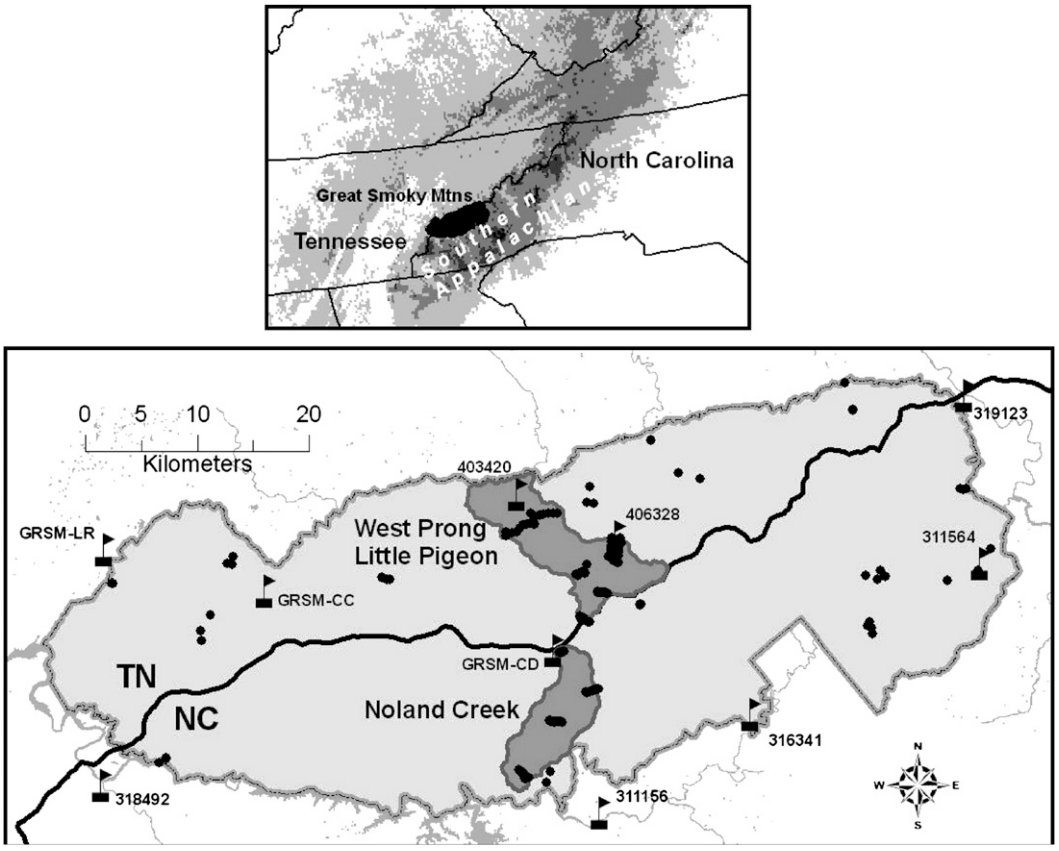

FIG. 1. (top) Location of GSMNP, in TN and NC, in the southern Appalachians. Elevations above 300 m are indicated in gray. (bottom) Two focal watersheds of the GSMNP Temperature Network (West Prong Little Pigeon and Noland Creek), location of 170 temperature dataloggers (circles) including 50-sensor validation dataset outside focal watershed boundaries, and locations of 10 surrounding weather stations (flagged rectangles; stations listed in Table A1).

lapse rates—in particular, in the winter (Shanks 1954; Busing et al. 2005). Regardless of elevation or season, GSMNP experiences high relative humidity above the tree canopy (80%–95%; Busing et al. 2005), and the near-ground air is saturated much of the year—in particular, away from ridges (based on unpublished data obtained by the author). Cloud cover is heavier and more persistent at high elevations, which also contributes to environmental lapse rates (Busing et al. 2005).

b. GSMNP Temperature Network

A preliminary study of the distribution of maximum and minimum daily temperatures with respect to landscape features of a single watershed was conducted in 2004. Twenty temperature dataloggers [HOBO H8 (Onset Computer Corporation of Bourne, Massachusetts)] mounted in waterproof enclosures 1 m above ground level were deployed across the Noland Creek watershed (Fig. 1), stratified coarsely by elevation, aspect, and ridge or streamside locations. Least squares regression analysis indicated significant effects of elevation, aspect, and stream proximity on July mean temperature, which became the basis for the subsequent parkwide network. In the spring of 2005, a permanent temperature sensor network was deployed in two focal watersheds and additional clusters of three sensors were spread throughout the park (Fig. 1). Two ~50-km^2 focal watersheds were chosen based on their near-complete coverage of the elevation gradient in GSMNP, the relative ease of access throughout each watershed, and their representation of different overall aspects. The Noland Creek watershed (in North Carolina; Fig. 2) ranges from 518 to 2024 m MSL, includes the highest elevation in the park, and has an overall southern aspect. The West Prong Little Pigeon (WPLP) watershed (in Tennessee; Fig. 3) ranges from 427 to 2009 m MSL with an overall northwestern aspect. Within each focal watershed, sensors were arrayed along six transects that began at the main stream channel and proceeded upslope to the top of the

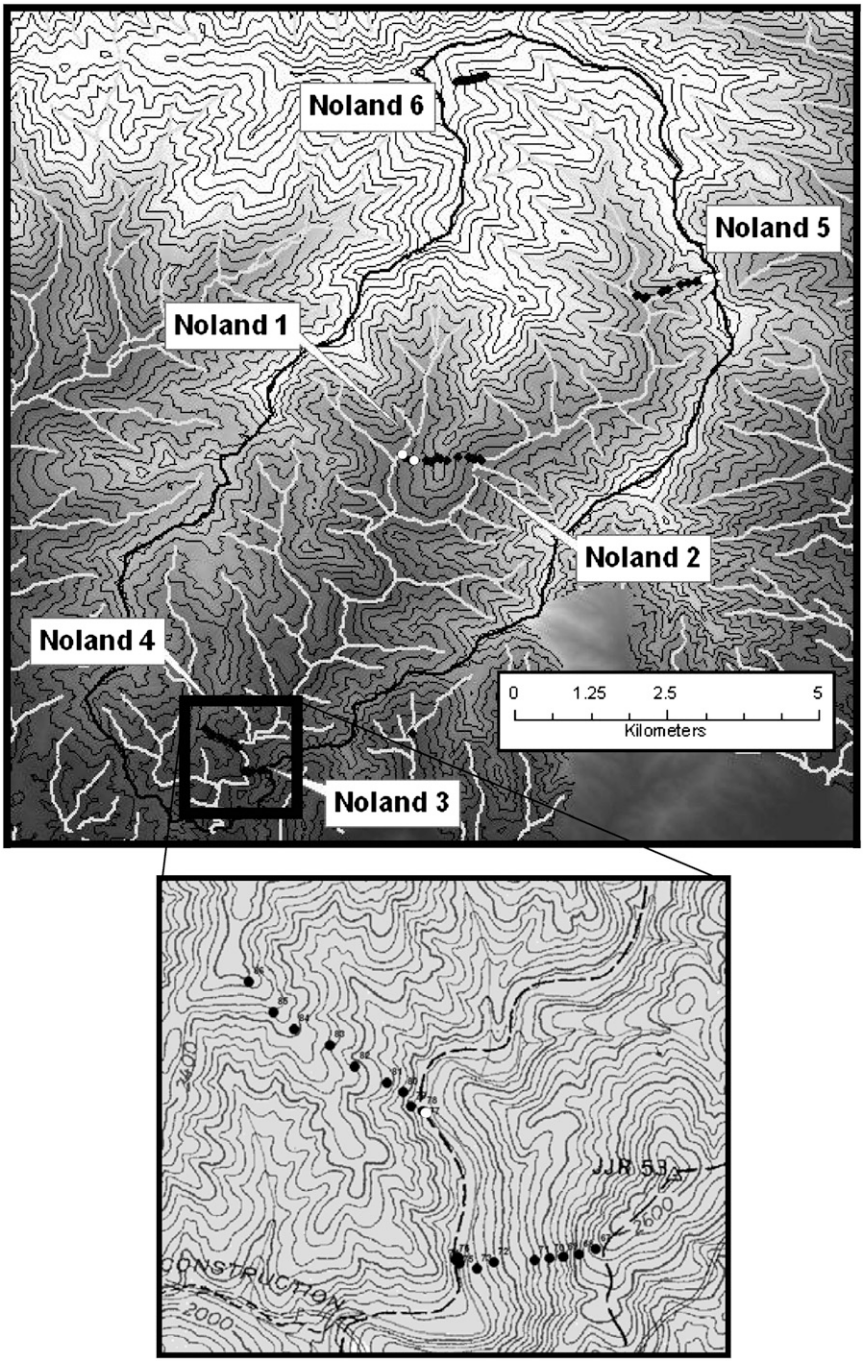

FIG. 2. (top) Layout of six temperature sensor transects in the Noland Creek (NC) watershed. Transects 1 and 2 are continuous but cover different opposing ridge sides. Transects 3 and 4 are oriented on facing hillslopes. (bottom) Transects 3 and 4, shown in greater detail. White dots indicate HOBO sensors that were excluded from model building, including two sensors on transect 1, one on transect 4, and three on transect 5.

nearest ridge, often the boundary of the watershed. Transects typically included 10 sensors each, corresponding to between-sensor distances of 50–500 m, depending on slope length. The six transects were further grouped into different overall aspects: for Noland Creek, this included three eastern- and three western-oriented transects (Fig. 2); for the more topographically complex WPLP watershed, this included northeastern

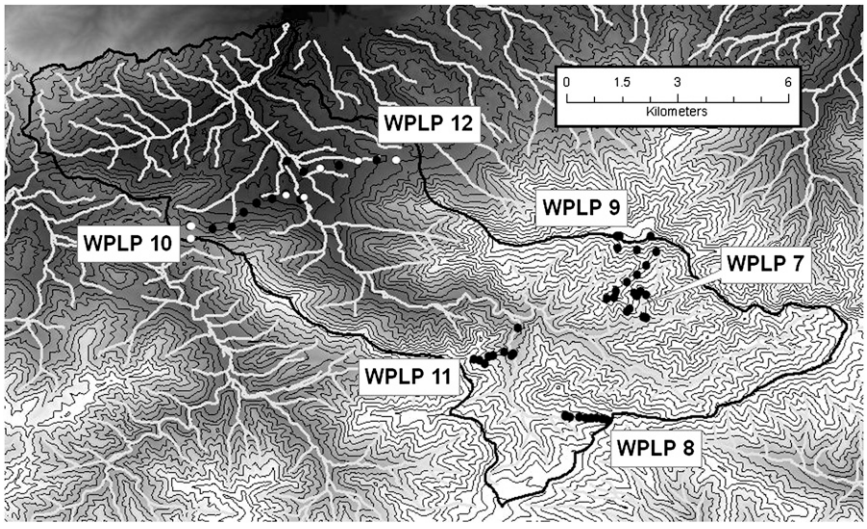

FIG. 3. Layout of six temperature sensor transects in the West Prong Little Pigeon (TN) watershed. Transects 7 and 9 are the lower and upper portions, respectively, of the Alum Cave trail to the summit of Mount Le Conte. White dots indicate HOBO sensors that were excluded from model building, including four sensors on transect 10 and three on transect 12.

versus southwestern orientations (Fig. 3). Each watershed initially included 60 sensors, grouped into six transects of two orientations, from low to high transect elevations. A set of 50 parkwide model validation sensors was deployed in the spring of 2005 to facilitate model extrapolation to the entire 2090-km^2 park, over a spatial extent of more than 80 km. Sensors were typically deployed in clusters of three and stratified by overall park region (north vs south; east, central, and west) and elevation (Fig. 1).

HOBO H8 loggers were redeployed in 20 of the 170 above locations of the temperature network. The remaining 150 locations were fitted with Thermocron Ibuttons [model DS1921G with a resolution of 0.5°C (Maxim Integrated Products, Inc., of Sunnyvale, California)]. At each location, an Ibutton was attached to the north side of a tree 1 m above ground level to minimize radiation forcing and was further protected from rain and radiation by enclosing it within a 12.7-mm schedule-40 polyvinyl chloride (PVC) cap mounted with PVC bracket, open at the bottom. A 1-m height was chosen for ease of deployment and maintenance and as a compromise between having a response height that is significant for trees, herbs, and aboveground animals and avoiding common animal disturbances such as ground foraging by hogs. All loggers were deployed by June of 2005 and recorded ambient temperature at 2-h intervals. The 2-h interval was chosen to maximize logger deployment duration (about 6 months) while keeping the error associated with estimation of true daily minima and maxima to approximately the 0.5°C resolution of the sensor, as determined by the preliminary dataset of hourly intervals (mean hourly change of ~0.3°C).

c. *Spatial modeling: Predictor variables*

The goal of a landscape-level model of temperature is to associate easily measured landscape features (e.g., elevation, slope, aspect, and topographic indices such as concavity and upslope catchment area) with processes that locally modify near-ground heat balance (e.g., radiation load, water content and evaporative load, and wind movement). A full review of the relationship between topographic features and microsite heat balance is outside the scope of this paper (see Geiger et al. 2003); described here are only the major topographic processes influencing near-ground temperature regimes and their GIS-derived proxy variables. Maximum daily temperature is driven by the daily duration and intensity of direct beam solar radiation (Cantlon 1953; Geiger et al. 2003; Chung and Yun 2004), which over uneven terrain is controlled by a surface's orientation (aspect) and slope, as well as shading by adjacent landforms (''hillshade''; Pierce et al. 2005) and overlying vegetation. Soil moisture and near-ground humidity are also critical parameters in site heat balance because of their influence on evaporation and transpiration. In wet sites, radiant energy in the morning dries surfaces before it warms them, leading to significantly cooler maximum daily temperatures in wetter locations (Dai et al. 1999). In contrast, minimum daily temperatures vary according to how cold air moves across land surfaces (katabatic winds) and are only indirectly related to daytime radiation

TABLE 1. Predictor variables for each mixed-effect multilevel regression model. Full descriptions of each variable are given in the appendix.

Variable	Description	Units	Range in GSMNP	Source or derivation
minSYN	Daily min temperature estimate from weather stations and lapse rate	°C	—	Regression of 10 synoptic weather values and ELEV
maxSYN	Daily max temperature estimate from weather stations and lapse rate	°C	—	Regression of 10 synoptic weather values and ELEV
RAD	Daily shortwave radiation	W m^{-2}	462–9394	r.sun (GRASS)
JDATE	Yearday (1 = 1 Jan 2005)	—	—	—
TOTRAD	Annual shortwave radiation	W m^{-2}	484 200–2 838 000	Annual sum of RAD
ELEV	Elevation (MSL)	m	256–2024	30-m digital elevation model
STRDST	Stream distance (log transformed)	m	0–1000	GIS based on stream coverage
TCI	Topographic convergence index (log transformed)	Unitless	1.26–25	GIS based on DEM (r.topidx in GRASS)

balances (Bergen 1969; Manins and Sawford 1979). The absence of direct radiation at night increases the importance of heat losses from longwave radiation, which is influenced by slope angle and the presence of overhead vegetation, and radiating heat gains from the ground, which in part connect nighttime and daytime temperatures. Just as for maximum temperature, soil moisture is an important part of site heat balance at night, buffering near-ground minimum temperatures from cold extremes (e.g., frost protection) and limiting the capacity of soils to act as a heat reservoir (Geiger et al. 2003).

For the purposes of modeling near-ground temperatures across landscapes, the principal elements are site radiation load, soil moisture levels, and cold-air drainage, in addition to elevation and properties of the ambient air mass. GIS-derived predictor variables corresponding to these factors are described in the appendix and are listed in Table 1. A 30-m digital elevation model (DEM) for GSMNP served as the basis for all topographically derived indices, analyzed in the Geographic Resources Analysis Support System (GRASS), version 5.4, GIS UNIX framework (GRASS Development Team 2006).

d. Spatial modeling: Model construction

A mixed-effect, multilevel modeling structure was used to predict daily sensor temperature (minimum and maximum) from regional weather station data and GIS-derived predictor variables (Table 1). Mixed-effects models are ideal for representing the covariance structure of grouped or clustered samples because they incorporate both fixed effects (known or repeatable environmental variables) and random effects (those associated with individual sampling units or clusters) within a common model structure (Pinheiro and Bates 2004). The multilevel model structure is particularly appropriate for modeling observations that are correlated in both space and time; temporal variation is nested within a single spatial location, and spatial variation can be assessed within and between spatial clusters. In this study, temperature data are structured in three nested levels. First, temperature varies from day to day at a single location; over the duration of this study, each sensor includes 488 observations (1 July 2005–31 October 2006) of daily minimum and maximum temperature (level one). Second, the mean temperature over those 488 observations at each site varies as a function of location within transects; sensors are clustered within transects, and transects typically include 10 unique spatial locations (level two). Third, the mean temperature of each transect varies as a function of overall transect position (including mean elevation and slope orientation), which is modeled at the between-transect level (12 transects; level three). In a mixed-model structure a random effect can be associated with each sample unit (here, days within locations, locations within transects, and whole transects); this has the advantage of excluding variance that cannot be attributed to environmental variables of interest (fixed effects) and thus can remove ''noise'' that would otherwise influence subsequent model extrapolation (only the fixed effects are used in model extrapolation and mapping).

A detailed description of the model fitting procedures for minimum and maximum temperature models is described in the online supplementary material in ''supplement A,'' along with the specification of final fitted models. Model fitting was performed with the R, version 2.3.1, software (see online at http://www.r-project.org/) using the ''nlme'' library (Pinheiro et al. 2006). Coefficients were fit through maximum likelihood, and terms were tested sequentially at each level using values of Akaike's information criterion (AIC) from log-likelihood tests (Burnham and Anderson 2002). Although spatial autocorrelation is addressed by random-effects terms

within clusters (transects), temporal autocorrelation of residuals was addressed by including a final term describing temporal correlation as exponential decay through time (the ''corCAR1'' correlation function in the nlme library). Preliminary analysis of all 120 model locations revealed that HOBO H8 sensors were consistently and unusually warmer than Ibuttons in similar locations, likely because of the full enclosure of these thermocouples within plastic boxes. To eliminate the error caused by different sensor designs, data from the 20 HOBO sensors were removed from subsequent analyses.

e. Model validation and mapping

To validate use of the model for the entire park, daily minimum and maximum temperatures for the set of 50 validation sensors spanning the spatial extent of GSMNP were predicted from final multilevel models of minimum and maximum temperatures and were compared with actual daily minimum and maximum values. Model bias (absolute difference between predicted and actual daily temperatures) and accuracy [mean absolute error (MAE), the difference between predicted and actual temperatures after making all observations positive] were estimated independently, and MAE was compared with a simple model that included only predictions based on daily lapse rates from the 10 weather stations.

Fixed-effect coefficients from final validated models of daily minimum and maximum temperature were extracted in R and were used to predict daily minimum and maximum temperatures of each 30-m pixel of GSMNP for the period for which the model was run, from July 2005 through October 2006. Maps were generated by vector processing of predictor variable maps in R 2.3.1 run within the GRASS 5.4 UNIX environment (Neteler and Mitasova 2004). Common temperature variables are available as Google Earth Keyhole Markup Language—Zipped (KMZ) files in the online supplemental material as ''supplement C.''

3. Results

a. Synoptic GSMNP climate patterns

From 1 July 2005 to 31 October 2006, regional temperatures exhibited seasonal minima in early January of 2006 and seasonal maxima in mid-August (2005) or mid-July (2006) (Fig. 4a). Daily minima were on average 13°C cooler than daily maxima at the lowest (''baseline'') elevations regardless of season (Fig. 4a), but fundamental differences in lapse rates for minimum and maximum temperatures, and the sensitivity of those lapse rates to season (Fig. 4b), produced different seasonal trajectories for temperature at different elevations. Minimum temperature lapse rates averaged -3.9°C km^{-1} over this period, did not vary systematically with season, and occasionally indicated whole-park temperature inversions where average minimum temperatures increased with elevation (Fig. 4b). Daily maximum temperature lapse rates were consistently higher than minimum rates (mean -6.8°C km^{-1}) and showed a strong seasonal trend of relatively high rates in summer and early autumn and low rates in winter (Fig. 4b). Lapse rate values showed less overall day-to-day variance in summer than in winter for both maximum and minimum temperatures.

b. Temperature variation within transects

1) MINIMUM DAILY TEMPERATURE

AIC tests of residuals from a linear mixed-effects model of site minimum temperatures as a function of elevation, averaged by month and grouped by transect, suggested stronger within-transect effects of (log transformed) stream distance (STRDST) than of topographic convergence index (TCI; see the appendix), effects that varied in intensity and direction depending on season. In warmer months, transects were consistently cooler near streams; sites 1000 m from streams could be 2°C or more warmer than streamside locations (Fig. 5; in particular note Noland transects 2–5 and WPLP transects 7, 8, and 11). Several high-elevation transects, however, exhibited opposite trends in some winter months (as shown by Fig. S1, available in the online supplementary materials as part of ''supplement B''), suggesting that stream proximity at the highest elevations could have a buffering effect of cooling sites in summer and warming sites in winter. Although TCI varied less within transects than STRDST because of a survey design explicitly stratified with STRDST, sites of higher moisture potential were significantly colder for transects with a range of TCI values (Fig. S2 of supplement B), with an effect again as high as 2°C even after accounting for STRDST. Differences in total annual radiation (TOTRAD) did not account for additional variation in minimum temperature at the within-transect level.

2) MAXIMUM DAILY TEMPERATURE

TOTRAD rather than STRDST or TCI was used to model residuals from a mixed-effects model of maximum temperatures as a function of elevation, again averaged by month and grouped by transect. AIC tests

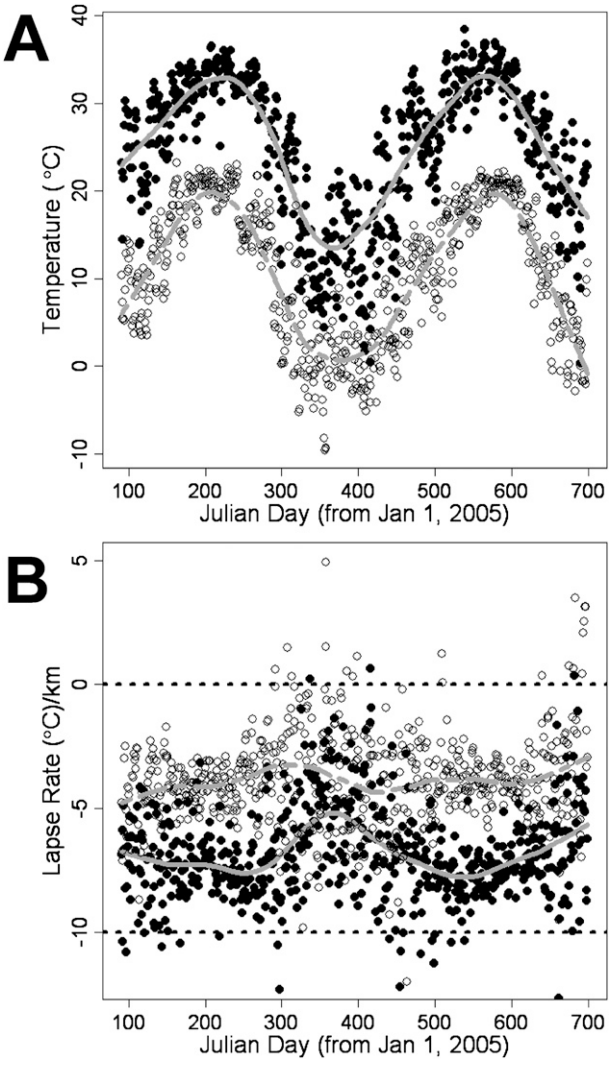

FIG. 4. Day-to-day variation in (a) baseline (projected sea level) temperature and (b) environmental lapse rates in the Great Smoky Mountains region from 1 Jul 2005 to 31 Oct 2006, estimated from 10 regional weather stations. Filled symbols describe maximum daily temperatures, open symbols are daily minima, and gray dashed and solid lines are locally weighted regressions of minimum and maximum datasets, respectively. Data were produced by daily intercept and slope estimates from least squares linear regression of daily minimum and maximum temperatures against station elevation. Horizontal dashed lines denote the free-air dry-adiabatic maximum lapse rate of $-9.8°C\ km^{-1}$ and the inversion region above $0°C\ km^{-1}$.

confirmed that within-transect effects of TOTRAD were significant but were not consistent among transects (Fig. 6). In winter, TOTRAD differences among sites within transects could alter maximum temperatures by more than 4°C (Fig. 6) but became minor in summer. STRDST accounted for additional residual variation in maximum temperature within some transects, by as much as 4°C even after accounting for elevation (ELEV) and TOTRAD differences (Fig. S3 of supplement B), but TCI did not in additional AIC tests.

c. *Multilevel temperature models across days and locations*

Descriptions of model building and results of significance testing in the mixed-effect framework are presented in online supplement A, grouped by regression level. Models predict the minimum or maximum temperature of site i on transect j on day t. Fitted model coefficients for fixed effects are listed in Table 2. Fixed and random effects of final (full) composite models include the following variables, listed by model.

1) MINIMUM TEMPERATURE

Day-to-day temperature fluctuations accounted for a large portion of model variance, and, in accord with this, synoptic temperature estimates corrected for daily lapse rates (minSYN) were strong predictors of minimum site temperatures in the composite model (Table 2). Nighttime temperatures were also indirectly warmed by site radiation balance (RAD) and exhibited additional seasonal trends that were not captured by weather station data [cosine and sine functions of yearday (JDATE); Table 2]. Effects of ELEV, STRDST, and TCI were strongly tied to overall synoptic temperatures and season (Table 2), consistent with within-transect patterns. As regional air masses warm, warming effects of stream proximity (inverse of STRDST) on nighttime temperatures decrease while the cooling effects of TCI increase. The indirect influence of RAD on minimum temperature was also reduced with higher regional temperatures but was accentuated by STRDST. Although broad-scale elevation effects are already included in the minSYN term, additional residual effects of ELEV are enhanced in a warmer atmosphere (Table 2). Random-effects terms identified with AIC tests included the effect of time within site and site within transect, the effect of minSYN between sites and between transects, and the effect of RAD between transects. The fitted intercept indicated that minimum ground-level temperatures under a canopy were 1.5°C warmer on average than those predicted by weather station measurements.

2) MAXIMUM TEMPERATURE

Synoptic temperature estimates from weather station data were significant but less important for predicting maximum temperatures than for minimum temperatures, and instead daily site radiation balance (RAD) and its interaction with synoptic temperatures (maxSYN) were the most powerful drivers of daytime site

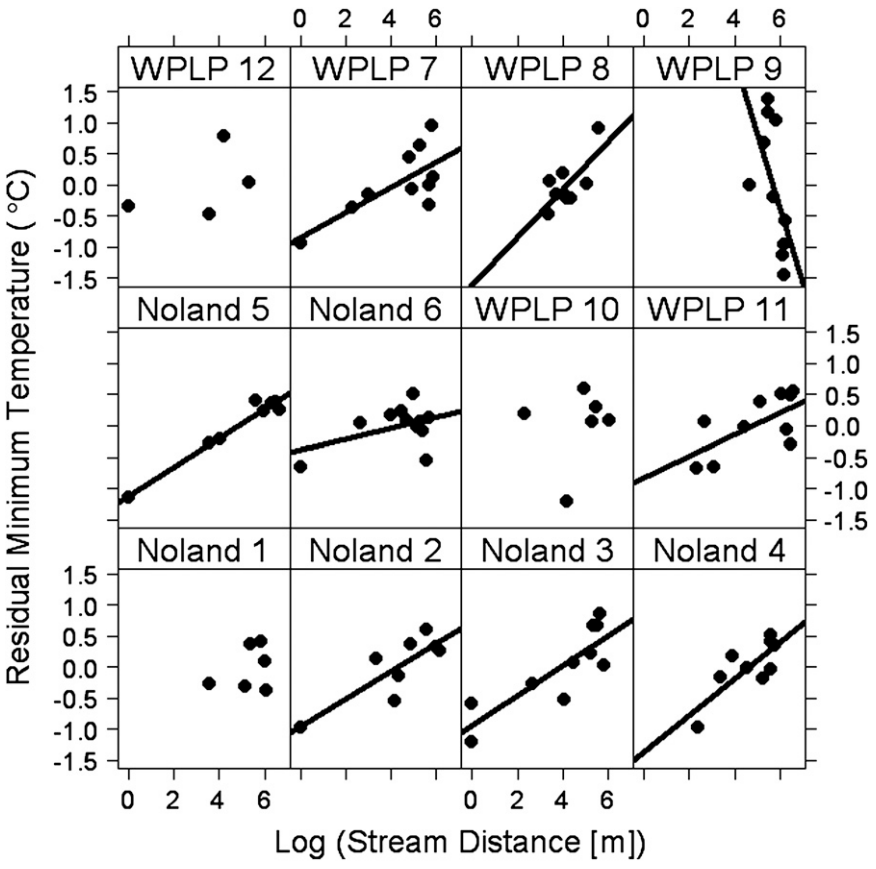

FIG. 5. Within-transect modeling of minimum daily temperature averaged over July 2005 and 2006 as a function of (log transformed) stream distance, expressed as residuals from a mixed-effect model including only elevation fit separately among transects. Lines are least squares regressions for transects exhibiting significant (significance level $P < 0.05$) relationships between residuals and STRDST.

temperatures (Table 2). Landscape-level effects of ELEV, STRDST, and TCI on maximum temperatures exhibited the same dependence on synoptic temperatures and season as did minimum temperatures, and effects of both ELEV and TCI decreased with RAD. Random-effects terms included the effect of time within site and site within transect, the effect of maxSYN between sites and between transects, and the effect of RAD between sites and transects. The fitted intercept indicated that near-ground maximum daily temperatures under mature forest canopies in GSMNP are substantially lower (more than 6°C) than weather station measurements.

d. Model performance and validation

Bias and accuracy statistics of the full minimum and maximum temperature models for the 50-sensor validation dataset spread out across all of GSMNP are presented in Table 3, including a comparison of the full model predictions with those derived from a model built from only daily weather station–derived baseline temperature and lapse rates (''synoptic only''). There was a strong and consistent bias in the synoptic-only model toward more extreme daily temperatures. On average, synoptic predictions were 1.8°C cooler at night and 2.2°C warmer during the day than actual temperatures of the validation sensors, effects that were particularly dramatic during the associated seasons of cold and hot weather (Table 3). There was no consistent bias in the full model (~0.1°C averaged over months for both minimum and maximum models). Predictions from the full model were accurate to within 1.6°C on average for minimum temperatures and 2.1°C on average for maximum temperatures, which varied significantly by month. Small MAEs were found for predictions of summer and early autumn temperatures for both minimum and maximum models, whereas most spring and November temperatures were more difficult to predict, with mean errors as high as 3.2°C for maximum temperatures (Table 3). Full model predictions were significantly

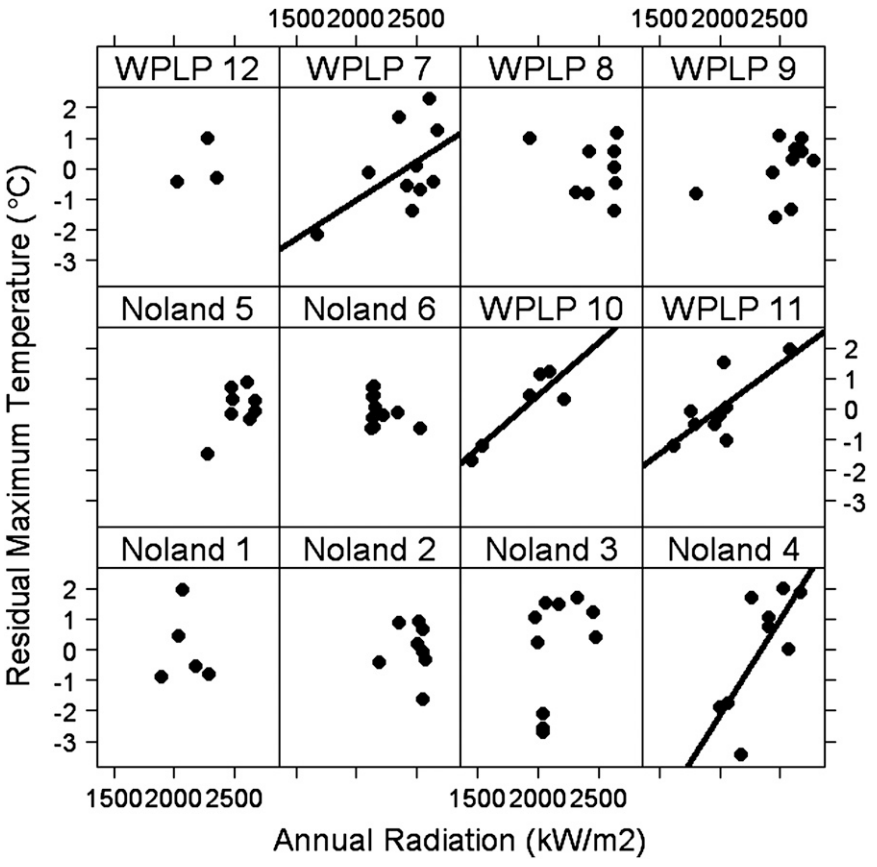

FIG. 6. Within-transect modeling of maximum daily temperature averaged over January 2006 as a function of total annual radiation, expressed as residuals from a mixed-effect model including elevation fit separately among transects. Lines are least squares regressions for transects exhibiting significant ($P < 0.05$) relationships between residuals and TOTRAD.

more accurate than synoptic-only predictions, however. Except for essentially no difference in the performance of the models in March and April, the full model described maximum temperatures about 1.1°C more accurately than did the synoptic-only model, and by more than 2°C during the summer months (Table 3). Minimum temperature estimates were on average 0.6°C more accurate for the full model, and this difference varied little by season.

e. Distribution of ground-level temperature in GSMNP

Maps of near-ground minimum and maximum temperatures for all of GSMNP at a 30-m resolution, using GIS maps of topographic variables and fixed-effect model coefficients of minimum and maximum temperatures (Table 2), are illustrated with two examples of mean January and July temperatures for 2006 (Fig. S4 of online supplement B). Viewed from a whole-park perspective, minimum temperatures appear to be more strongly coupled to elevation than are maximum temperatures. Finer-scale perspectives of these maps offer better views of the influence of landscape features on site temperature regimes (Fig. S5 of online supplement B). Maximum temperatures exhibited high finescale variance largely in response to landform complexity and consequent patterns of direct radiation levels (Fig. S5a), and minimum temperatures were more closely associated with ridge and valley positions (Fig. S5b). Minimum temperatures for the full extent of GSMNP were well correlated with elevation ($R^2 = 0.91$; where R is correlation coefficient), while maximum temperatures were only partially related to elevation ($R^2 = 0.51$; Fig. 7).

4. Discussion

a. Finescale variation of temperature within complex landscapes

A major contribution of the results from the GSMNP Temperature Network presented here is the demonstration of high ground-level climate variation over very

TABLE 2. Model summaries of fitted fixed effects from multilevel regression models of minimum and maximum daily temperature, 1 Jul 2005–31 Oct 2006. Variables are defined in Table 1. Model terms were fit using maximum likelihood, and terms were tested sequentially with AIC values of competing models. The *P* values reported below are from likelihood ratio tests and were not used for model building. Random-effects terms are noted in the text and are specified in online supplement A. Here, one asterisk indicates $P < 0.05$, two are for $P < 0.01$, and three indicate $P < 0.001$; SE is standard error, and df is degrees of freedom.

Factor	Value	SE	df	*t* value	*P*
		Min daily temperature			
(Intercept)	1.468 971 3	0.948 386 1	45 610	1.55	
minSYN	1.024 991 1	0.030 792 5	45 610	33.29	***
RAD	0.000 365 0	0.000 099 0	45 610	3.69	***
cos(0.0172 × JDATE)	0.895 064 2	0.311 230 8	45 610	2.88	***
sin(0.0172 × JDATE)	0.349 251 4	0.121 161 1	45 610	2.88	***
ELEV	0.000 546 0	0.000 618 7	86	0.88	
STRDST	−0.113 092 9	0.091 935 5	86	−1.23	
TCI	−0.382 764 7	0.205 051 0	86	−1.87	
minSYN:RAD	−0.000 009 5	0.000 000 8	45 610	−11.83	***
cos(0.0172 × JDATE):ELEV	−0.001 349 9	0.000 148 7	45 610	−9.08	***
sin(0.0172 × JDATE):ELEV	−0.000 552 2	0.000 044 4	45 610	−12.44	***
cos(0.0172 × JDATE):STRDST	0.163 324 3	0.039 649 1	45 610	4.12	***
sin(0.0172 × JDATE):STRDST	0.036 194 6	0.012 166 8	45 610	2.97	**
cos(0.0172 × JDATE):TCI	−0.211 256 3	0.083 352 9	45 610	−2.53	**
sin(0.0172 × JDATE):TCI	−0.195 174 7	0.042 211 2	45 610	−4.62	***
minSYN:ELEV	−0.000 141 7	0.000 012 6	45 610	−11.27	***
minSYN:STRDST	0.020 539 6	0.002 224 8	45 610	9.23	***
minSYN:TCI	−0.026 960 4	0.010 507 7	45 610	−2.57	*
RAD:ELEV	−0.000 000 2	0.000 000 1	45 610	−2.41	*
RAD:STRDST	0.000 028 4	0.000 013 6	45 610	2.08	*
		Max daily temperature			
(Intercept)	−6.732 644 0	2.497 935 4	45 608	−2.70	**
maxSYN	0.646 659 0	0.059 067 3	45 608	10.95	***
RAD	0.003 131 0	0.000 347 5	45 608	9.01	***
cos(0.0172 × JDATE)	8.072 879 0	1.013 590 1	45 608	7.96	***
sin(0.0172 × JDATE)	−0.607 760 0	0.278 220 2	45 608	−2.18	*
TOTRAD	−0.000 004 0	0.000 000 5	85	−7.96	***
ELEV	0.005 511 0	0.000 986 5	85	5.59	***
STRDST	−0.195 415 0	0.082 636 7	85	−2.36	*
TCI	0.251 769 0	0.892 781 4	85	0.28	
maxSYN:RAD	−0.000 026 0	0.000 001 2	45 608	−21.41	***
cos(0.0172 × JDATE):TOTRAD	−0.000 001 0	0.000 000 3	45 608	−4.11	***
sin(0.0172 × JDATE):TOTRAD	0.000 001 0	0.000 000 1	45 608	7.06	***
cos(0.0172 × JDATE):ELEV	−0.003 189 0	0.000 217 6	45 608	−14.65	***
sin(0.0172 × JDATE):ELEV	−0.001 212 0	0.000 061 8	45 608	−19.63	***
cos(0.0172 × JDATE):STRDST	0.307 341 0	0.045 195 5	45 608	6.80	***
sin(0.0172 × JDATE):STRDST	0.126 769 0	0.014 928 8	45 608	8.49	***
cos(0.0172 × JDATE):TCI	0.106 299 0	0.274 672 8	45 608	0.39	
sin(0.0172 × JDATE):TCI	−0.058 406 0	0.074 308 9	45 608	−0.79	
maxSYN:ELEV	−0.000 026 0	0.000 032 7	45 608	−0.81	
maxSYN:TOTRAD	0.000 000 0	0.000 000 0	45 608	5.11	***
maxSYN:STRDST	0.036 336 0	0.003 312 1	45 608	10.97	***
RAD:ELEV	−0.000 001 0	0.000 000 2	45 608	−5.64	***
RAD:TCI	−0.000 191 0	0.000 129 1	45 608	−1.48	

short distances, largely as the product of topographic complexity and its influence on the critical heat balance factors of incident radiation, soil water content, and local air drainage. Near-ground temperatures in forested ecosystems also systematically differ from well-mixed above-canopy air, being both significantly cooler during the day and significantly warmer at night than temperatures indicated by open-site weather station sensors. Although the protective influence of a heavy forest canopy on diurnal temperature extremes of near-ground air has been found repeatedly in forest microclimate studies (Hough 1945; Hursh 1948; Parker 1995; Morecroft et al. 1998), the consistent and significant discrepancy indicated in this study (about 2°C less for

TABLE 3. Bias and MAE of model predictions of full multilevel temperature models, relative to a model based only on daily weather station data and lapse rate (''synoptic only''), grouped by month. Bias is the difference between predicted and actual daily temperatures, averaged by month for 50 validation sensors. MAE is the difference between predicted and actual temperatures after making all observations positive. The ''Δ accuracy'' is the MAE difference between synoptic-only and full models. ''Overall'' statistics are means across months. Each statistic represents about 1500 observations (50 sensors over 30 days).

	Month	Jan	Feb	Mar	Apr	May	Jun	Jul	Aug	Sep	Oct	Nov	Dec	Overall
							Min temperature							
Bias	Synoptic only	−1.90	−1.86	−2.21	−2.26	−1.81	−1.70	−1.12	−1.24	−1.73	−2.06	−1.93	−2.06	−1.82
	Full model	−0.05	0.66	0.27	−0.31	0.25	−0.04	0.21	0.05	0.05	0.05	0.15	0.26	0.13
MAE	Synoptic only	2.28	2.42	2.54	2.63	1.99	1.86	1.39	1.37	1.91	2.32	2.99	2.36	2.17
	Full model	1.82	1.81	1.82	1.81	1.38	1.23	1.09	0.95	1.28	1.57	2.30	1.51	1.55
	Δ accuracy	0.46	0.61	0.72	0.82	0.61	0.63	0.30	0.43	0.63	0.75	0.69	0.85	0.62
							Max temperature							
Bias	Synoptic only	2.13	1.02	−0.25	0.84	2.10	3.09	3.62	3.59	3.23	2.44	2.10	2.09	2.17
	Full model	0.13	0.39	−0.50	−0.21	0.65	0.15	0.03	−0.07	0.11	−0.31	−0.67	−0.26	−0.05
MAE	Synoptic only	3.13	2.69	2.86	3.20	2.90	3.48	3.75	3.66	3.34	2.90	2.96	2.84	3.14
	Full model	2.48	2.38	2.89	3.17	2.13	1.69	1.42	1.26	1.42	1.69	2.51	1.96	2.08
	Δ accuracy	0.64	0.32	−0.03	0.03	0.77	1.79	2.33	2.41	1.93	1.20	0.45	0.88	1.06

both daily extremes—equivalent to nearly 300-km latitudinal variation in mean temperatures in the eastern United States) suggests climate-based studies of forest organisms must take into account the bias of weather station temperature data (Shanks and Norris 1950).

The magnitude of near-ground temperature variation over short distances indicated in transect-level variance in the GSMNP Temperature Network will be significant to environmental biologists accustomed to using elevation as a simple indicator of climate regime in montane systems. Although elevation and mean January minimum temperatures are well correlated in the mapped product of the entire park ($R^2 = 0.91$), minimum January temperature variation for a fixed level of elevation still approached 2°C, similar to the magnitude of cold-air variation along stream-to-ridge transects after accounting for elevation. Because the range of mean minimum January 2006 temperature for the full park was only 8°C, such finescale variation independent of elevation becomes considerable. Maximum temperatures exhibited even greater independence from elevation (see also Ashcroft et al. 2008). Only about one-half of the full-park variation in mean July 2006 maximum temperatures could be accounted for by elevation, and transect-level variation (over a few hundred meters) was as high as 4°C. For perspective, this is about the same maximum annual temperature difference as New Orleans, Louisiana, and St. Louis, Missouri—cities separated by 1000 km.

b. Landscape features that drive local temperature regimes

The spatial structure of maximum (daytime) near-ground temperature in GSMNP is driven largely by topographic differences in direct-beam radiation exposure, a relationship that has been well documented in both open, arid landscapes (Shreve 1924) and the more protected forested landscapes of the eastern deciduous forest (Shanks and Norris 1950; Cantlon 1953; Desta et al. 2004). The magnitude of the radiation effect in this study is perhaps surprising given that near-ground environments in GSMNP are as wet as any in the eastern United States and most sites are well protected by several tree and shrub strata (Whittaker 1956). However, many low-elevation ridge-top communities in GSMNP have been severely impacted by pine beetle infestations and subsequent canopy tree blowdowns (Nicholas and White 1984), including ridge-top sites of three of the four lowest-elevation transects used in this study. It is thus likely that part of the radiation effect quantified here is accounted for by a sparser tree canopy on ridges rather than above-canopy differences in radiation load. Indeed, the current study makes no attempt to separate topography-related effects (TCI, STRDST, RAD) from effects caused by differences in vegetation structure that are inevitably correlated with topography for both climatic and nonclimatic reasons. Additional sample stratification by forest disturbance history could isolate the indirect effects of forest-stand history on near-ground climate. In addition, landscapes with more variable land cover in addition to forest types (e.g., wetlands, fields, and talus slopes) will require more explicit sample stratification by land cover type.

The spatial structure of minimum near-ground temperatures in GSMNP is driven by local topography and a tighter coupling to elevation. Such topographic effects may indicate both cold-air drainage downslopes at night and the moister conditions of more concave landforms, especially protected cove sites near perennial stream locations (Geiger et al. 2003). Both stream proximity

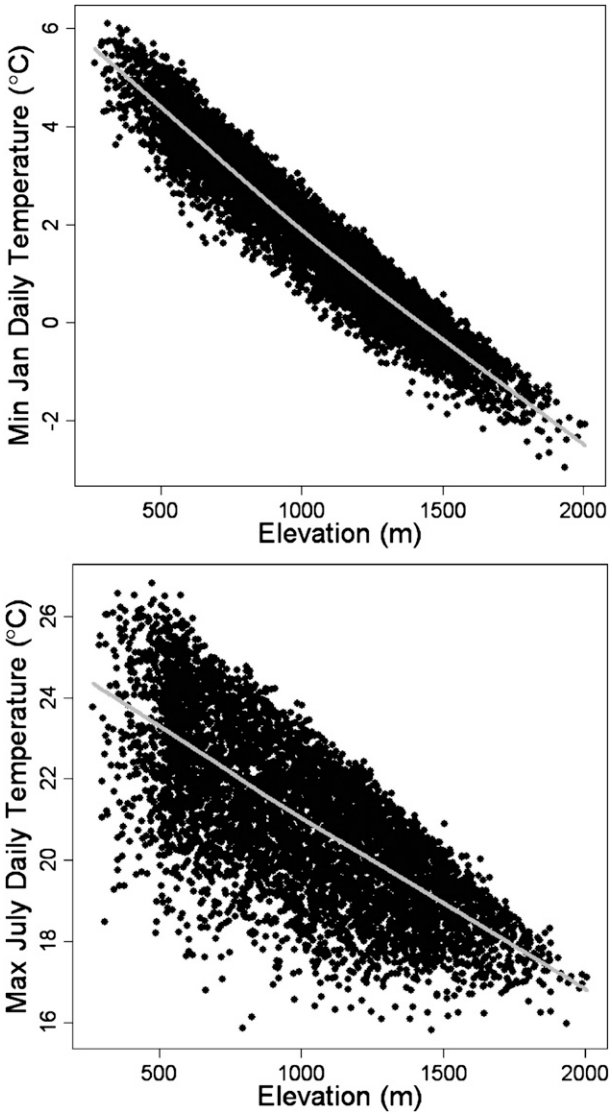

FIG. 7. Relationships between elevation and (top) average minimum daily temperature in January 2006 and (bottom) average maximum daily temperature in July 2006, derived from the full extent of GSMNP. Lines are locally weighted regressions. Lapse rate for January minimum temperature is 4.7°C km^{-1}.

(STRDST) and TCI were strongly associated with the topographic effect on minimum temperatures, but despite TCI being a more common indicator of soil moisture status (Lookingbill and Urban 2004), STRDST proved a better predictor of within-transect minimum temperature variance. The stronger effects of soil moisture than cold-air drainage are also indicated by the greater tendency of STRDST effects to shift to a warming effect near streams in winter at some locations. Spatial differences in water regimes have been indicated as important factors in GSMNP temperatures before: Shanks (1954) suggested that the extreme water surplus of high elevations causes delayed high-elevation warm-up in spring (over a month after low-elevation spring warming) and slower diurnal temperature fluctuations. In addition, the tendency of lapse rates to increase in summer during the highest annual temperatures may indicate that drier low-elevation temperatures are more strongly coupled to regional airmass properties and heat up as predicted, whereas hot air masses cannot easily elevate water-saturated high-elevation temperatures—in particular, when temperature is measured near the saturated forest floor. If true, then lower-elevation habitats and exposed ridges may be far more sensitive to future atmospheric warming than those of high elevations and protected streamsides, suggesting the intriguing possibility that the overall climate gradient in GSMNP—responsible for much of the park's remarkable biotic diversity—may actually increase in the coming decades.

Effects of all three dominant mechanisms of landscape-scale near-ground temperature variation—radiation, soil moisture, and cold-air drainage—varied significantly with season and with properties of the regional air mass, in addition to interactions of elevation with both synoptic and seasonal variables. Such interactions were enough to change even the direction of some effects, as with the influence of cold-air drainage on lapse rate and the buffering effect of streams on temperature extremes. Interactions of topographic effects with season and regional air masses have two major ramifications for the study of mountain climates: 1) the model coefficients determined in this study for GSMNP should not necessarily hold for other regions dominated by different synoptic climate systems, even given a similar landscape structure, and 2) sites within GSMNP do not maintain relative temperature differences described on any given day or month over the course of an entire year. The first point suggests that the model coefficients presented in Table 2 may hold for other landscapes in the southern Appalachians but may be inappropriate to apply elsewhere. The second point has great import for the study of montane species distributions in relation to near-ground microclimate, in that single-season temperature measurements will not necessarily reflect true differences in temperature regimes between sites or species (Cantlon 1953; Shanks 1954; Saunders et al. 1998).

c. Microclimate considerations in GSMNP

GSMNP protects a major biological hotspot in North America (Stein et al. 2000) and is generally considered the historical epicenter of the eastern deciduous forest biome (Braun 1950; Whittaker 1956). The driving force behind this status has long been thought to be based on

geography (southern extent of high peaks in the Eastern United States) and topography (extreme elevation gradient), both of which infer a great diversity of contemporary and historical climates within a relatively small area. Shanks (1954, 1956) remains one of the few studies of climate for the area, and it established baseline information on climate differences at different elevations, in particular as it reflects differences in precipitation and evapotranspiration (Shanks 1954). The few subsequent studies (Busing et al. 2005; Gaffin et al. 2007) involved only a handful of weather stations in and near GSMNP (see also Bolstad et al. 1997).

To this general backdrop of colder, wetter conditions at higher elevations, the current study adds much needed detail and brings climate data down to the level of most of the park's biota. Advances provided by this study of the GSMNP Temperature Network include 1) a strong signal of greater temperature extremes along ridges and buffered microclimates in the wettest locations, implicating additional factors in biotic differences between ridge and cove communities; 2) high capacity for finescale spatial variance in near-ground temperatures, especially those caused by differences in site insolation; 3) much more limited diurnal and seasonal temperature fluctuations under a forest canopy than those suggested by surrounding weather station measurements; and 4) a strong decoupling of elevation and daytime temperatures and, to a more limited extent, nighttime temperatures. The indication that soil moisture plays a significant role in near-ground temperatures by buffering sites from temperature extremes suggests that the important historical role of the region as an ecological refuge during past climate shifts may be due to both a highly dissected topography and the ability of protected coves to withstand major temperature fluctuations.

d. Refinement of temperature mapping techniques

The incorporation of high-resolution landscape features in a spatial climate model provides significant advances in describing local temperature regimes that organisms experience, but the increasing availability of spatial data in a GIS framework suggests climate models could incorporate additional variables that were not explicitly addressed in this study. In particular, finescale remote sensing data such as daily cloud cover, snow cover, and seasonal albedo changes at high elevations, and various leaf area and productivity indices may further reduce day-to-day error in site temperatures, especially given the importance of leaf phenology in deciduous forest stands and the contribution of both cloud and leaf cover to near-ground maximum temperatures. Development of high-resolution water balance maps, in concert with the near-ground temperature modeling presented here, would allow a more mechanistic examination of the dependence of temperature on water balance and vice versa; however, such finescale hydrologic studies are logistically problematic for large spatial extents. Model accuracy for daily site minimum and maximum temperatures will also improve with sensors of greater resolution and shorter measurement intervals. Because the observation error contributed by these factors in the current study (combined effects estimated between 0.5° and 1°C) approaches the accuracy limit detected for estimating monthly averaged minimum temperatures (Table 3), significant increases in model accuracy with the inclusion of additional landscape factors will require substantial reductions in observation error.

Of particular interest to climate change researchers is the ability of the high-resolution mapping approach described here to be extrapolated to past and future climates. Because the model is tied to regional weather station data that are often available for much of the twentieth century, summaries of spatial temperature predictions can be extrapolated back in time based on model coefficients from contemporary weather data. In a similar way, the model described here can be extrapolated forward in time using current synoptic warming predictions (e.g., Alley et al. 2007) to downscale regional climate predictions to a spatial resolution relevant to most migrating organisms. For example, seasonal coarse-resolution predictions (e.g., 1 km^2) from regional models can be used as the synoptic estimates of minimum and maximum temperatures that serve as level-1 inputs to the model rather than weather station values (see online supplement A). However, it is important to note that the same caveats concerning spatial model extrapolation to regions of different landscape or airmass properties also apply to temporal extrapolation, in that ground-level climates of the distant past or far-off future may have very different relationships to topographic factors. Nonetheless, with the prospect of linking landscape-scale species distribution data to recent high-resolution climate histories, and extrapolating such models to expected future climates, this approach offers a promising means of increasing the precision of bioclimatic change predictions to the scales most relevant for local ecosystem management (Araújo et al. 2005).

Acknowledgments. I gratefully acknowledge J. Weiss for statistical help and E. Fridley for field assistance; K. Woods, J. Mayer, and M. Clauser for providing additional field help; K. Langdon, J. Renfro, and GSMNP park staff for providing logistical support; and T. Jobe, P. White, and T. Lookingbill for providing thoughtful

discussion. This study was supported by the National Parks Ecological Research Fellowship program, a partnership between the National Park Service (NPS), the Ecological Society of America, and the National Park Foundation, and funded through a generous grant from the Andrew W. Mellon Foundation.

APPENDIX

Derivation of Spatial Model Predictor Variables

a. Daily radiation values

Total annual direct-beam radiation was calculated for each 30-m pixel in GRASS using the ''r.sun'' algorithm (Neteler and Mitasova 2004). With a supplied DEM, r.sun uses date, latitude, slope orientation, slope angle, and shading from local topography to calculate daily intercepted solar irradiance (W m^{-2}) based on Earth–sun geometry. Preliminary analyses using other radiation proxies, including transformed aspect (Beers et al. 1966), hillshade maps, and potential relative radiation (Pierce et al. 2005), suggested that the r.sun routine is a more accurate descriptor of radiation distribution and is easier to calculate in the GRASS environment.

b. Local topographic indices

Preliminary analyses describing temperature distribution as a function of landscape-scale water and airflows explored the predictive ability of a suite of standard topographic and hydrologic DEM-derived indices, including relative slope position (Wilds 1996), tangential and plane curvature (Wilds 1996), distance from stream (log transformed; Lookingbill and Urban 2003), and topographic convergence index, which estimates site water potential by calculating a site's upslope catchment area and correcting for local slope (Beven and Kirkby 1979). Because these variables measure similar topographic properties, they are partially correlated; furthermore, only STRDST and TCI were consistently related to local variation in temperature regimes in preliminary models, and values of STRDST and TCI have the desirable property of relative ease of interpretation. Within a single precipitation regime, sites of higher TCI values are wetter (Beven and Kirkby 1979), and STRDST should also capture evening airflows that follow stream courses (Lookingbill and Urban 2003). TCI was calculated with the GRASS algorithm ''r.topoidx.'' Note that the use of TCI to describe potential soil moisture is only accurate for areas that receive similar precipitation regimes and have similar soil properties; for this reason TCI was used to predict temperatures only within single transects.

c. Seasonal effects

A continuous cosine–sine function with a period of 365 days was used as a proxy for seasonal variation in local temperature regimes that could not be accounted for by variation in daily synoptic input. Significant seasonal effects in this category could include several unmeasured environmental attributes, including canopy phenology, seasonal patterns of cloud cover and snowfall albedo, and regular changes in atmospheric turbidity and water content. The well-established seasonal variation in environmental lapse rates (Shanks 1954; Bolstad et al. 1998; Busing et al. 2005) is accounted for in daily synoptic input. Use of the periodic function to describe seasonal effects allows for the fitting of only two parameters to describe season (coefficients for cosine and sine functions; see online supplement A).

d. Synoptic weather station baseline values

Ten weather stations within or immediately adjacent to GSMNP were selected to provide baseline daily maximum and minimum temperatures and derivation of daily minimum and maximum lapse rates (Fig. 1). Three stations are operated by the Air Resources Division of the National Park Service (http://www2.nature.nps.gov/air),

TABLE A1. Weather stations within and nearby GSMNP providing daily synoptic maximum and minimum temperature inputs (ID is identifier; UTM denotes universal transverse Mercator coordinates in meters for zone 17).

Station name	Type	Station ID	UTM easting	UTM northing	Elev (m)
Cades Cove	NPS air quality	GRSM-CC	247 870	3 943 410	564.0
Clingmans Dome	NPS air quality	GRSM-CD	273 540	3 938 130	2033.0
Look Rock	NPS air quality	GRSM-LR	233 550	3 947 030	793.0
Oconaluftee	NCDC cooperative	316341	291 110	3 932 370	621.8
Bryson City 2	NCDC cooperative	311156	277 660	3 923 600	618.1
Mount Le Conte	NCDC cooperative	406328	279 060	3 948 230	1979.1
Gatlinburg 2 SW	NCDC cooperative	403420	270 300	3 951 990	443.2
Cataloochee	NCDC cooperative	311564	311 620	3 945 850	807.7
Waterville 2	NCDC cooperative	319123	310 150	3 960 750	438.9
Tapoco	NCDC cooperative	318492	233 240	3 926 050	338.9

and the remaining seven stations are National Climatic Data Center (NCDC) cooperative stations (Table A1). All NCDC stations use thermocouples of the Maximum–Minimum Temperature System style in shielded minitowers (1–2 m above ground level), except for two (Mount Le Conte and Tapoco) that contain liquid maximum–minimum thermometers in cotton region shelters. The three NPS stations use thermocouples on significantly higher towers (4, 10, and 13 m above ground level for Cades Cove, Look Rock, and Clingmans Dome, respectively). For each day of the model, maximum and minimum temperatures were regressed against elevation for each site to produce daily baseline temperatures (intercept) and lapse rates (slope), which served as model input for each 30-m pixel based on elevation (minSYN and maxSYN; Table 1).

REFERENCES

Alley, R. B., and Coauthors, 2007: Summary for policymakers. *Climate Change 2007: The Physical Basis,* S. Solomon et al., Eds., Cambridge University Press, 1–18.

Araújo, M. B., W. Thuiller, P. H. Williams, and I. Reginster, 2005: Downscaling European species atlas distributions to a finer resolution: Implications for conservation planning. *Global Ecol. Biogeogr.,* **14,** 17–30.

Ashcroft, M. B., L. A. Chisholm, and K. O. French, 2008: The effect of exposure on landscape scale soil surface temperatures and species distribution models. *Landscape Ecol.,* **23,** 211–225.

Barry, R. G., 1992: *Mountain Weather and Climate*. 2nd ed. Routledge, 402 pp.

——, 2005: Alpine climate change and cryospheric responses: An introduction. *Climate and Hydrology in Mountain Areas*, C. de Jong, D. Collins, and R. Ranzi, Eds., John Wiley and Sons, 1–4.

Beers, T. W., P. E. Dress, and L. C. Wensel, 1966: Aspect transformation in site productivity research. *J. For.,* **64,** 691–692.

Bergen, J. D., 1969: Cold air drainage on a forested mountain slope. *J. Appl. Meteor.,* **8,** 884–895.

Beven, K. J., and M. J. Kirkby, 1979: A physically based, variable contributing area model of basin hydrology. *Hydrol. Sci. Bull.,* **24,** 43–69.

Bolstad, P. V., B. J. Bentz, and J. A. Logan, 1997: Modelling microhabitat temperature for *Dendroctonus ponderosae* (Coleoptera: Scolytidae). *Ecol. Modell.,* **94,** 287–297.

——, L. Swift, F. Collins, and J. Régnière, 1998: Measured and predicted air temperatures at basin to regional scales in the southern Appalachian Mountains. *Agric. For. Meteor.,* **91,** 161–176.

Braun, E. L., 1950: *Deciduous Forests of Eastern North America*. Blakiston, 596 pp.

Breshears, D. D., J. W. Nyhan, C. E. Heil, and B. P. Wilcox, 1998: Effects of woody plants on microclimate in a semiarid woodland: Soil temperature and evaporation in canopy and intercanopy patches. *Int. J. Plant Sci.,* **159,** 1010–1017.

Burnham, K. P., and D. R. Anderson, 2002: *Model Selection and Multimodel Inference: A Practical Information-Theoretic Approach*. 2nd ed. Springer-Verlag, 488 pp.

Busing, R. T., L. A. Stephens, and E. E. C. Clebsch, 2005: Climate data by elevation in the Great Smoky Mountains: A database and graphical displays for 1947–1950 with comparison to long-term data. U.S. Geological Survey Data Series Rep. DS 115, 33 pp.

Cantlon, J. E., 1953: Vegetation and microclimates on north and south slopes of Cushetunk Mountain, New Jersey. *Ecol. Monogr.,* **23,** 241–270.

Chung, U., and J. I. Yun, 2004: Solar irradiance-corrected spatial interpolation of hourly temperature in complex terrain. *Agric. For. Meteor.,* **126,** 129–139.

Cogbill, C. V., P. S. White, and S. K. Wiser, 1997: Predicting treeline elevation in the southern Appalachians. *Castanea,* **62,** 137–146.

Dai, A., K. E. Trenberth, and T. R. Karl, 1999: Effects of clouds, soil moisture, precipitation, and water vapor on diurnal temperature range. *J. Climate,* **12,** 2451–2473.

Desta, F., J. J. Colbert, J. S. Rentch, and K. W. Gottschalk, 2004: Aspect induced differences in vegetation, soil, and microclimatic characteristics of an Appalachian watershed. *Castanea,* **69,** 92–108.

Dodson, R., and D. Marks, 1997: Daily air temperature interpolated at high spatial resolution over a large mountainous region. *Climate Res.,* **8,** 1–20.

Gaffin, D. M., D. G. Hotz, and T. I. Getz, cited 2007: An evaluation of temperature variations around the Great Smoky Mountains National Park and their associated synoptic weather patterns. [Available online at http://www.srh.noaa.gov/mrx/research/smokytemp/smokytemp.php.]

Geiger, R., R. H. Aron, and P. Todhunter, 2003: *The Climate near the Ground*. 6th ed. Rowman and Littlefield, 584 pp.

GRASS Development Team, 2006: Geographic Resources Analysis Support System (GRASS) software. Version 6.1.0. [Available online at http://grass.itc.it.]

Hough, A. F., 1945: Frost pocket and other microclimates in forests of the northern Allegheny Plateau. *Ecology,* **26,** 235–250.

Hursh, C. R., 1948: Local climate in the Copper Basin of Tennessee as modified by the removal of vegetation. U.S. Department of Agriculture Circular 774, 38 pp.

Iverson, L. R., and A. M. Prasad, 1998: Predicting abundance of 80 tree species following climate change in the eastern United States. *Ecol. Monogr.,* **68,** 465–485.

Lookingbill, T. R., and D. Urban, 2003: Spatial estimation of air temperature differences for landscape-scale studies in montane environments. *Agric. For. Meteor.,* **114,** 141–151.

——, and ——, 2004: An empirical approach towards improved spatial estimates of soil moisture for vegetation analysis. *Landscape Ecol.,* **19,** 417–433.

Manins, P. C., and B. L. Sawford, 1979: Katabatic winds: A field case study. *Quart. J. Roy. Meteor. Soc.,* **105,** 1011–1025.

Morecroft, M. D., M. E. Taylor, and H. R. Oliver, 1998: Air and soil microclimates of deciduous woodland compared to an open site. *Agric. For. Meteor.,* **90,** 141–156.

Neteler, M., and H. Mitasova, 2004: *Open Source GIS: A GRASS GIS Approach*. 2nd ed. Springer, 401 pp.

Nicholas, N. S., and P. S. White, 1984: The effect of the southern pine beetle on fuel loading in yellow pine forests of Great Smoky Mountains National Park. National Park Service Southeast Regional Office, 31 pp.

Parker, G. G., 1995: Structure and microclimate of forest canopies. *Forest Canopies,* M. D. Lowman and N. M. Nadkarni, Eds., Academic Press, 73–106.

Parker, J., 1952: Environmental and forest distribution of the Palouse Range in northern Idaho. *Ecology,* **33,** 451–461.

Pierce, K. B., T. R. Lookingbill, and D. L. Urban, 2005: A simple method for estimating potential relative radiation (PRR) for

landscape-scale vegetation analysis. *Landscape Ecol.,* **20,** 137–147.

Pinheiro, J. C., and D. M. Bates, 2004: *Mixed-Effects Models in S and S-Plus*. Springer-Verlag, 528 pp.

——, ——, S. DebRoy, and D. Sarkar, 2006: NLME: Linear and nonlinear mixed effects models. R package version 3.1-73. [Available online at http://cran.r-project.org/web/packages/nlme/index.html.]

Saunders, S. C., J. Chen, T. D. Drummer, and T. R. Crow, 1998: Modeling temperature gradients across edges over time in a managed landscape. *For. Ecol. Manage.,* **117,** 17–31.

Shanks, R. E., 1954: Climates of the Great Smoky Mountains. *Ecology,* **35,** 354–361.

——, 1956: Altitudinal and microclimatic relationships of soil temperature under natural vegetation. *Ecology,* **37,** 1–7.

——, and F. H. Norris, 1950: Microclimatic variation in a small valley in eastern Tennessee. *Ecology,* **31,** 532–539.

Shreve, F., 1912: Cold air drainage and plant distribution. *Plant World,* **15,** 110–115.

——, 1924: Soil temperatures as influenced by altitude and slope exposure. *Ecology,* **5,** 128–136.

Stein, B. A., L. S. Kutner, and J. S. Adams, 2000: *Precious Heritage: The Status of Biodiversity in the United States*. Oxford University Press, 399 pp.

Thornton, P. E., S. W. Running, and M. A. White, 1997: Generating surfaces of daily meteorological variables over large regions of complex terrain. *J. Hydrol.,* **190,** 214–251.

Trivedi, M. R., P. M. Berry, M. D. Morecroft, and T. P. Dawson, 2008: Spatial scale affects bioclimate model projections of climate change impacts on mountain plants. *Global Change Biol.,* **14,** 1089–1103.

Urban, D. L., C. Miller, P. N. Halpin, and N. L. Stephenson, 2000: Forest gradient response in Sierran landscapes: The physical template. *Landscape Ecol.,* **15,** 603–620.

Whittaker, R. H., 1956: Vegetation of the Great Smoky Mountains. *Ecol. Monogr.,* **26,** 1–80.

Wilds, S., 1996: Gradient analysis of the distribution of flowering dogwood (*Cornus florida* L.) and dogwood anthracnose (*Discula destructiva* Redlin.) in western Great Smoky Mountains National Park. M.A. thesis, Dept. of Ecology, University of North Carolina, 151 pp.